J. Environ. Eng. Manage., 17(5), 311-318 (2007)

REMOVAL OF METHOMYL PESTICIDE BY ADSORPTION USING NOVEL HYPERCROSSLINKED POLYMER OF MACRONET MN-100

Chiung-Fen Chang,[1] Ching-Yuan Chang,[2,*] Kuo-En Hsu,[2] Wolfgang Höll[3] and Pen-Chi Chiang[2]

[1]Department of Environmental Science and Engineering
Tunghai University
Taichung 407, Taiwan
[2]Graduate Institute of Environmental Engineering
National Taiwan University
Taipei 106, Taiwan
[3]Forschungszentrum Karlsruhe
Institute for Technical Chemistry
D-76021 Karlsruhe, Germany

Key Words: Adsorption, hypercrosslinked polymer, methomyl, equilibrium, kinetics

ABSTRACT

Carbamates are the most commonly used insecticides in Taiwan, in which methomyl takes the top-ranking of aggregate sales. Due to the long half-life of methomyl in ground water, the stringent pesticide standard of water bodies and protection of human health, the treatment technologies of contaminated water bodies are required urgently. Novel hypercrosslinked polymer (Macronet MN-100 denoted as MN-100) with large surface area and microporous pore volume possesses great potential for the removal of pesticide from the aqueous solution. This study attempts to apply an adsorption process to remove methomyl from aqueous environment using MN-100. The adsorption equilibrium and kinetics of methomyl on MN-100 were predicted by using Langmuir and Freundlich isotherms, and simple kinetic models (e.g., Lagergren pseudo-first-order, pseudo-second-order and Elovich rate equations). Furthermore, the effect of pH value of the solutions on adsorption capacity of methomyl also has been investigated in this study.

INTRODUCTION

Pesticides are worldwide used to prevent the croppers, forestry and horticulture from the damages of insects, diseases, fungi and other pests, to adjust the growth of the plants, or to increase the yields of the croppers. However, it has to be taken into account that only a small part of the applied pesticides reaches its final destinations, the biological targets. The residual pesticides are still toxicologically active. These residual pesticides remain in the environment and must be destructed in the ecosystems to prevent accumulation or contamination. Therefore, pesticides are essential parts of xenobiotics brought into the environment by the human activities. Further, the most potential sources of risks can be found with the manufacturing plants, which may emit pesticides resulting in a large-scale soil and groundwater contamination [1].

Depending on the chemical compositions of pesticides, they exhibit different extents of toxicity for humans and animals. In addition, some pesticides have been found to affect the nervous systems of humans and animals and even have carcinogenic effects. It has been reported by Smulders et al. [2] that the carbamate pesticides inhibit the brain receptors and affect different subtypes of neuronal nicotinic receptors. According to European Community Drinking Water Directive, the standards for the individual pesticide and the sum of all pesticides are 0.1 and 0.5 ppb, respectively, which are both much more stringent than health-based minimum level set by the World Health Organizations and the US Environmental Protection Agency (USEPA) [3]. In order to meet the stringent pesticide standard of water bodies and protect human health, therefore, it is deemed that the treatment technology of contaminated water bodies is required urgently.

Over the past century, many processes have been developed and successfully applied for separating the substance from the fluid stream and purifying mix-

*Corresponding author
Email: cychang3@ntu.edu.tw

tures of substances. Adsorption is commonly recommended as one of the best available control technologies to recover or treat the volatile organic compounds from the waste streams and drinking water [4]. For water and wastewater treatment, applications of activated carbon (AC) to remove toxic organics have established an incomparable record of success as both effective and reliable [5]. Numerous publications in literature on adsorption of the organics on AC have been available in the past (for example, references 6-17). However, due to the expensive regeneration and fragile properties of AC, potential adsorbents such as polymeric resins were synthesized to replace AC.

For the non-ionic polymeric resins, according to the physical structures [18], they are classified as gel-type, macroporous (macroreticular) and hypercrosslinked (co-)polymers, in which the latter two are commonly used in water treatment. Furthermore, due to the high surface area and special functional groups tagged to the tail of the polymeric chains, hypercrosslinked polymers are expected to possess high adsorption capacity. Streat and Sweetland [19-23], and Tai et al. [24] had investigated the applications of Hypersol-Macronet^{TM} (i.e., Macronet) on the removal of organic pollutants and pesticides, and metal ions from aqueous solutions, indicating that Macronets have highly applicable potential for the adsorption process of the wastewater treatment.

Carbamates are the most commonly used insecticides in Taiwan, with methomyl taking the top-ranking of aggregate sales of carbamates [25]. Therefore, in this paper, the investigation of adsorption behaviors of methomyl, such as adsorption equilibrium and kinetics on novel hypercrosslinked polymer (Macronet MN-100 denoted as MN-100) were presented. Further, the stability of methomyl and the physicochemical characteristics of MN-100 were also investigated.

MATERIALS AND METHODS

1. Adsorbent

MN-100 was used as the adsorbent in this study. The physicochemical characteristics of MN-100 were characterized 1) using laser diffraction particle size analyzer (LS 230 with Fluid Volume Module, Beckman Coulter) for the mean particle size, 2) Accupyc 1330 (Micromeritics) for true density, 3) scanning electron microscopy (SEM, Hitachi S800) for surface image, and 4) electrophoresis (Zeta-Sizer 3000, Malvern) for zeta potential. The pretreatment of the adsorbent comprised of three sequential steps: washed by distilled water, dried by centrifuge (CN-2060, Hsiangtai) under 5000 rpm for 20 min, and then wetted in the specific wetting solutions under vacuum, prior to the subsequent adsorption experiments.

2. Preparation of Methomyl Solution

A stock solution of methomyl of 1 g L^{-1} was prepared by dissolving 0.2 g methomyl (technical material, supplied by TungFong Ltd. Co., Taiwan) in 200 mL acetonitrile solvent (reagent grade, Merck, Darmstadt, Germany). Then it was stored in the teflon-stoppered brown glass bottle. For the subsequent use, the stock solution was diluted to the specific concentrations with de-ionized water (18 MΩ cm) treated via Milli-Q.

3. Analytical Measurements

For measurements of adsorption equilibria and adsorption kinetic experiments of single-component of methomyl in a completely stirred tank reactor (CSTR), all samples were filtrated through a 0.22 μm membrane prior to the analysis, and then measured by means of high performance liquid chromatography (HPLC) with UV detector (Lab Allence). The concentrations were standardized with reagent-grade methomyl (Riedel-de Haën, Seelze, Germany). The wavelength used in HPLC was fixed at 233 nm.

4. Adsorption Kinetic Experiments

Adsorption kinetic experiments were conducted in a CSTR. A basket reactor was adopted to this system to avoid the attrition of adsorbent, which may be encountered in the slurry reactor. Various stirring speeds (N_r) from 500 to 800 rpm were beforehand examined, in order to ensure completely mixing and to reduce the film resistance to a minimum. The results show that as N_r was higher than 700 rpm, the effect of film mass transfer resistance was reduced substantially. Therefore, N_r of following experiments was fixed at 800 rpm to assure that the internal mass transfer resistance was predominantly important for the adsorption kinetics.

The ratio of adsorbent mass to solution volume was 250 g m^{-3} and the temperature was adjusted and controlled at 298 K. The initial concentrations of methomyl (C_0) were from 1 to 20 g m^{-3}. The experiments were stopped until reaching adsorption equilibrium (i.e., concentrations of filtrate did not change more than 3%). The amounts of methomyl adsorbed on MN-100 were calculated from the equilibrium concentrations under various C_0 to establish the adsorption isotherm. The effect of pH value of solution on adsorption capacity of methomyl on MN-100 was investigated by the means of bottle-point method with shaker shaken for 30 h at fixed temperature of 298 K. The specific amount adsorbed in all experiments was calculated using

$$q_e = \frac{(C_0 - C_e)V_L}{m_s} \quad (1)$$

where q_e is the adsorbate loading (g kg^{-1}) in the solid at equilibrium; C_e is the equilibrium concentration of methomyl (g m^{-3}); V_L is the volume of the aqueous solution; and m_S is the mass (g) of adsorbent used in the experiment.

RESULTS AND DISCUSSION

1. Characterizations of Physicochemical Properties of MN-100

The physicochemical characteristics of MN-100 measured in this study are presented in Table 1. The Langmuir specific surface area of MN-100 is 1097 m^2 g^{-1}, which can compete with the commercial AC, F-400 (Filtrasorb 400, Chemviron, European operation of Calgon Carbon Corperation), e.g., 1391 m^2 g^{-1} [26]. Further, the micropore area and average pore diameter are 571 m^2 g^{-1} (i.e., 91% of that of F-400) and 22 Å, respectively, indicating that MN-100 indeed is one of high potential adsorbents. Figure 1 illustrates the laser diffraction particle size analysis of MN-100. The results show that the median particle size of MN-100 is about 677 μm and the distribution of particle size is rather uniform.

Figure 2 presents the adsorption and desorption isotherms of N_2 at 77 K on MN-100. It is seen that the adsorption isotherm of N_2 for the portion with adsorbed volume below or near 250 cm^3 g^{-1} STP belongs to Type I of the Brunauer, Deming, Deming and Teller classification [27] with well-defined plateaus, interpreting that the pores of MN-100 are microporous. With increasing N_2 adsorbed volume (i.e., the relative pressure of adsorption system close to 1), the shape of adsorption isotherm changes to Type II, standing for that MN-100 also possesses the mesoporous structure. Besides, the adsorption-desorption curves could not overlap well, showing that the hysteresis loop exists. According to International Union of Pure and Applied Chemistry classification [28], the hysteresis loop with nearly parallel branches resembles Type H4 and represents the existence of slit-shaped pores.

SEM graphs of the surface structures of MN-100 are illustrated in Fig. 3. The shape of MN-100 is essentially spherical (Fig. 3a). With the increasing power, SEM pictures display more rough and irregular surface structures of MN-100. Up to the magnifying power of 30 k, the SEM image shows that the pore structure of MN-100 is made up of crosslink of polymeric matrices, resulting in high micropore surface.

Table 1. Physical properties of adsorbent MN-100 used in the adsorption experiments

Property		Value
Average particle size[a], d_P (mm)		0.677
Specific external surface area[b], a_S (m^2 kg^{-1})		12.14
Particle true density[c], ρ_S (kg m^{-3})		1097
Apparent particle density[d], ρ_P (kg m^{-3})		730
Particle porosity[e], ε_P		0.33
Surface area[f] (m^2 g^{-1})	Langmuir, A_L	1097
	BET, A_B	815
Micropore area[g] (m^2 g^{-1})		571
Pore volume (cm^3 g^{-1})	Total, V_t	0.458
	Micro-, V_i	0.266
	Meso-[h], V_e	0.142
	Macro-[h], V_a	0.050
Average pore diameter[i] (Å)		22
Zeta potential (pH_{PZC})		5

a. Analyzed using LS 230 Fluid Module.
b. Assumed as sphere and calculated using $a_s = 6/(\rho_P \times d_P)$
c. Analyzed using Accupyc 1330, Micromeritics.
d. Calculated using $1/((1/\rho_S)+V_t)$. V_t = total pore volume per unit mass of adsorbent.
e. Calculated using $1 - (\rho_P/\rho_S)$.
f. Analyzed using ASAP2010, Micromeritics.
g. Calculated using t-method.
h. Calculated using $V_t - V_i = V_e + V_a$, with Barrett, Joyner and Hanlenda (BJH) adsorption pore distribution, which gives the proportions of mesopore to macropore volumes.
i. Calculated using $4V_t/A_B$.

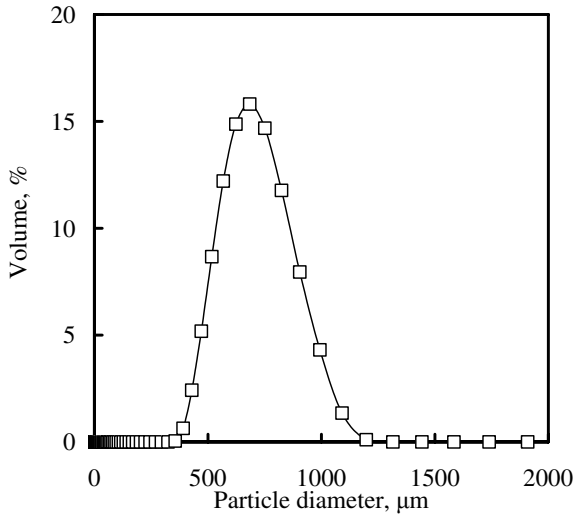

Fig. 1. Differential volume vs. particle diameter of MN-100. □: Experimental data.

2. Effect of pH Value of Solution on Adsorption Capacity

The chemical name of methomyl is S-methyl N-(methylcarbamoyloxy) thioacetimidate and the molecular weight is 162. According to the physicochemical properties of methomyl reported in Hazardous Substances Data Bank [29], the hydrolysis half-life of methomyl in aqueous environment depends on the pH value of the solution. Therefore, the effect of pH value of the solution on methomyl was investigated with the results presented in Fig. 4. In the pH range of 2 to 8,

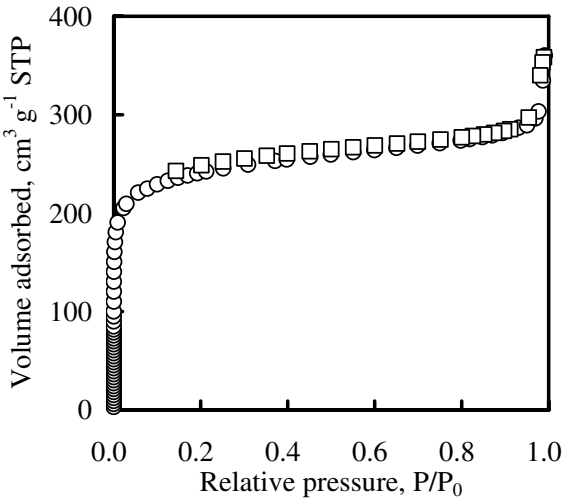

Fig. 2. Adsorption (○) and desorption (□) isotherms of N_2 at 77 K for MN-100. ○ and □: Experimental data.

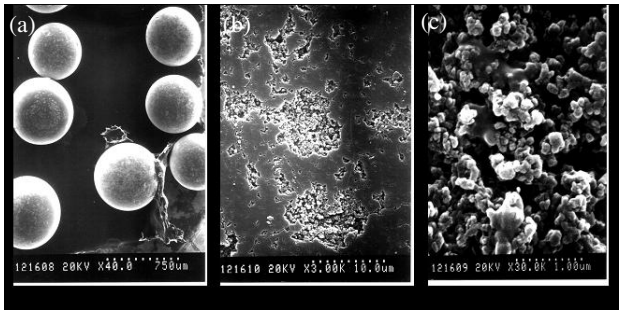

Fig. 3. SEM pictures of MN-100. (a). ×40; (b). ×3 k; (c). ×30 k.

the methomyl is rather stable. In contrast, when the pH value raises to 10, the residual amount of methomyl is only 12% of the original. Moreover, at high pHvalue of 12, methomyl is completely degraded to other compounds, interpreting that methomyl is degraded quite substantially in the basic solutions. Therefore, the effect of pH value on adsorption capacity was examined in the pH range of 2-8. As illustrated in Fig. 4, the adsorption capacity decreases with increasing pH value, indicating that the lower pH value of solution enhances the adsorption of methomyl. MN-100 is a weak base anion resin. Its pH_{PZC} (point of zero charge) is 5, as shown in Fig. 5. The adsorption of methomyl on MN-100 may be mainly due to dispersion forces and polarization of π electrons (electron-rich portion of the adsorbate). As the pH value of the solution is lower than pH_{ZPC} of MN-100 of 5, the surface of MN-100 exhibits positive charge and possesses highly positive sites, possibly resulting in promoting the adsorption capacity of methomyl on MN-100.

3. Adsorption Equilibrium

Adsorption isotherms with two adjustable pa-

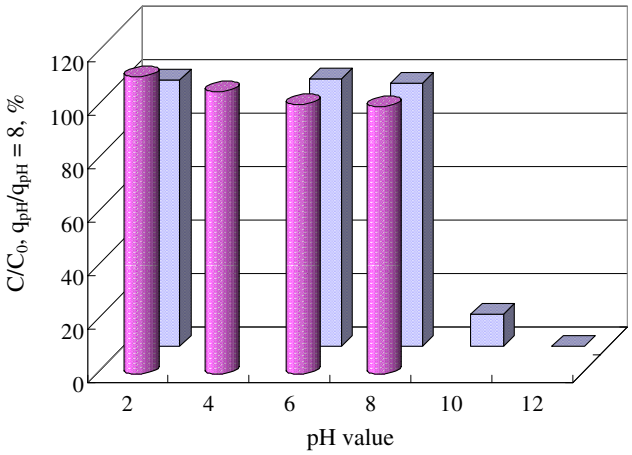

Fig. 4. Effect of pH value on degradation and adsorption capacity of methomyl on MN-100. The units of y axis for square (designated as C/C_0) and cylindrical bars (designated as q_{pH}/q_{pH} = 8, the ratio of adsorption capacity at various pH to that at pH = 8) are both %. The experiments were conducted applying bottle-point method shaken for 24 h. The initial concentration of methomyl (C_0) is 13 g m^{-3}, the volume of solution (V_L) is 0.2 L and the mass of MN-100 (m_S) is 0.1 g.

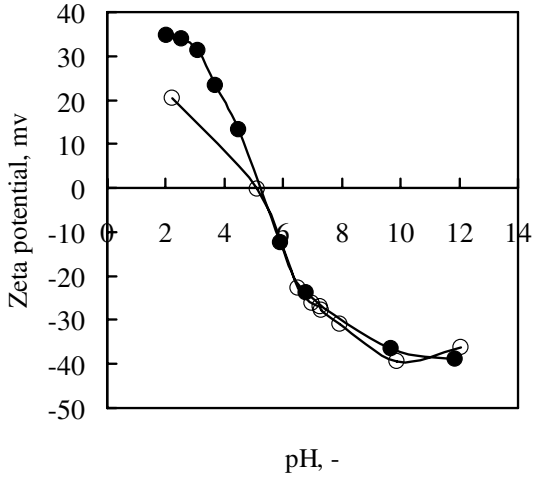

Fig. 5. Zeta potential of MN-100 as a function of pH value. ○ and ●: Ion strength = 0.01 and 0.1 N NaCl.

rameters such as Langmuir and Freundlich equations were used to describe the adsorption isotherm data of methomyl. The mathematical relationship of Langmuir and Freundlich isotherms are expressed as in Eqs. 2 and 3, respectively.

$$q_e = \frac{q_L K_L C_e}{1 + K_L C_e} \quad (2)$$

$$q_e = k_F C_e^{1/n_F} \quad (3)$$

In Eq. 2, q_e and C_e are the adsorbate concentrations in solid and liquid phases at equilibrium, respec-

Table 2. Values of adsorption isotherm parameters and correlation coefficients (r^2)[a] of adsorption of methomyl on MN-100

System	Langmuir isotherm			Freundlich isotherm		
	q_L (g kg^{-1})	K_L (m^3 g^{-1})	r_L^{2b}	k_F ((g kg^{-1}) (g m^{-3})$^{-1/n_F}$)	n_F	r_F^{2b}
Single-component of methomyl	21.6	1.22	0.966	9.52	2.09	0.988

a. The units for C_e and q_e are g m^{-3} and g kg^{-1}, respectively.

b. $r_L^2$and r_F^2 are correlation coefficients for linear regression fittings of experimental data via Langmuir and Freundlich isotherms, respectively.

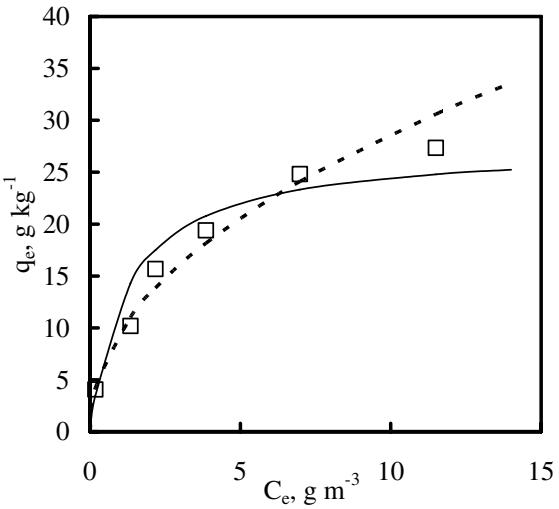

Fig. 6. Predictions using Freundlich isotherm (---) and Langmuir isotherm (—) for adsorption of methomyl on MN-100. □: Experimental data. q_e and C_e: Equilibrium concentrations of methomyl in solid and liquid phases.

tively. q_L and K_L are the Langmuir isotherm constants, of which the former expresses the monomolecular coverage of the surface of the adsorbent, while the latter stands for equilibrium constant. In Eq. 3, k_F and n_F are the Freundlich equilibrium constants, which represent the adsorption capacity and strength of adsorption, respectively. For a favorable adsorption, the value of n_F is greater than 1.

Both of the constants of adsorption isotherms can be determined via applying linear regression of the adsorption isotherm data. The results are shown in Table 2 and Fig. 6. The values of q_L and K_L for adsorption of methomyl on MN-100 are 21.6 g kg^{-1} and 1.22 m^3 g^{-1}, respectively. Judging by the value of n_F (i.e., 2.09) in the Freundlich isotherm, we note that the use of MN-100 to remove methomyl from the aqueous solution is favorable. Further, the correlation coefficients (i.e., r_L^2 = 0.966 and r_F^2 = 0.988) indicate that both Langmuir and Freundlich isotherms can well describe the adsorption of methomyl on MN-100 in the entire experimental range.

4. Adsorption Kinetics

The traditional models of adsorption kinetics usually encompass a complicated mathematical computation to acquire the related mass transfer and diffusion coefficients of the models, such as external and internal mass transfer coefficients [8,30]. Therefore, for the simplicity, the global kinetic expressions based on lumped analyses of adsorption kinetic data such as Lagergren pseudo-first-order (Eq. 4), pseudo-second-order (Eq. 5) [31] and Elovich (Eq. 6) [32-33] rate equations, are applied to interpret the adsorption kinetics in the study. The mathematic expressions of various models mentioned above are as follows.

$$\frac{dq_t}{dt} = k_{e1}(q_e - q_t) \tag{4}$$

$$\frac{dq_t}{dt} = k_{e2}(q_e - q_t) \tag{5}$$

$$\frac{dq_t}{dt} = a_E \exp(-b_E q_t) \tag{6}$$

where q_t and q_e are the adsorbate concentrations in the solid at time t and at equilibrium; k_{e1}, k_{e2} and a_E and b_E are the rate constants of the corresponding rate equations.

By means of using the same initial condition (q_t = 0 at t = 0), Eqs. 4-6 can be integrated as shown in Eqs. 7-9. Equation 9 can be further simplified under the condition of $a_E b_E t \gg 1$, as presented in Eq. 10.

$$\ln(q_e - q_t) = \ln(q_e) - k_{e1}t \tag{7}$$

$$\frac{t}{q_t} = \frac{1}{k_{e2}q_e^2} + \frac{t}{q_e} \tag{8}$$

$$q_t = \frac{1}{b_E}\ln(a_E b_E) + \frac{1}{b_E}\ln(t + t_0) \tag{9}$$

$$q_t = \frac{1}{b_E}\ln(a_E b_E) + \frac{1}{b_E}\ln(t) \tag{10}$$

The parameters of Eqs. 7, 8 and 10 obtained and the comparisons of experimental and predicted results are presented in Tables 3-4 and Fig. 7, respectively. Furthermore, the determination coefficient (R^2) is used to evaluate the applicability of the three models for adsorption kinetics of methomyl on MN-100, as given in Eq. 11.

$$R^2 = 1 - \left[\frac{\sum(y_e - y_c)^2}{\sum(y_e - y_m)^2}\right] \tag{11}$$

where y_e, y_c and y_m are the experimental and predicted

Table 3. Parameters and determination coefficient (R^2) of adsorption of methomyl on MN-100 employing various global kinetic models

Initial concentration	Lagergren equation			Pseudo-second-order equation			Elovich rate equation			
C_0 (g m^{-3})	r^2	k_{e1} (h^{-1})	R^2	r^2	k_{e2} (kg g^{-1} h^{-1})	R^2	r^2	a_E (g $kg^{-1}h^{-1}$)	b_E (kg g^{-1})	R^2
1.2	0.961	0.060	-0.502	0.999	0.093	0.972	0.994	6.87	1.590	0.991
3.9	0.960	0.063	0.169	0.995	0.027	0.956	0.991	14.69	0.624	0.988
8.7	0.972	0.049	0.185	0.996	0.012	0.966	0.992	17.83	0.315	0.988
13.2	0.989	0.059	0.529	0.992	0.008	0.930	0.979	24.03	0.251	0.979
18.4	0.972	0.055	0.527	0.991	0.007	0.938	0.983	25.48	0.231	0.983

Table 4. Comparison of equilibrium capacities (q_e) of adsorption of methomyl on MN-100

Initial concentration	Experimental data		Predicted results of q_e (g kg^{-1})			
C_0 (g m^{-3})	C_e (g m^{-3})	q_e (g kg^{-1})	Langmuir	Freundlich	Langergren	Pseudo-second-order
1.2	0.18	4.07	3.88	4.18	2.49	4.15
3.9	1.35	10.19	13.45	10.98	7.54	10.53
8.7	3.85	19.40	17.82	18.16	13.75	19.80
13.2	6.98	24.82	19.34	24.11	20.30	25.71
18.4	11.50	27.35	20.17	30.62	22.51	28.01

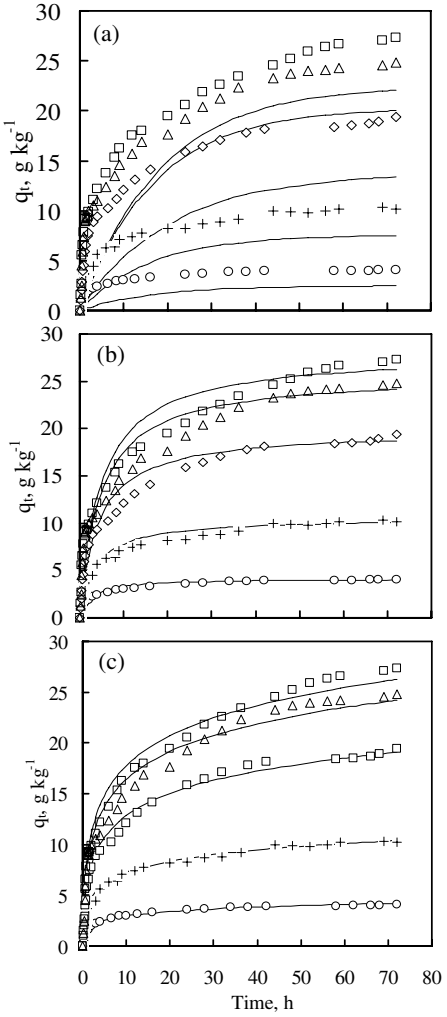

Fig. 7. Adsorption kinetics of methomyl on MN-100 at various C_0 in CSTR system by (a) pseudo-first-order, (b) pseudo-second-order, and (c) Elovich rate equations. ○, ＋, ◇, △ and □: C_0 = 1.2, 3.9, 8.7, 13.2 and 18.4 g m^{-3}, respectively. (—): Predictions.

data, and the average of the experimental values, respectively.

According to Eqs. 7, 8 and 10 along with their corresponding linear regression fittings, the parameters of individual rate equations were obtained with high correlation coefficient (r^2 of three models > 0.95). However, only the fittings of pseudo-second-order and Elovich rate equation gave high R^2, reflecting that the Lagergren pseudo-first-order equation is not suitable to describe the adsorption kinetics of methomyl on MN-100. Furthermore, comparing with the values of q_e obtained from the prediction of pseudo-second-order equation and experimental data also shows good agreement and supports its applicability. The value of the rate constant k_{e2} of the pseudo-second-order equation generally decreases with increasing C_0, interpreting that the higher concentration of methomyl results in the lower adsorption rate constant. The higher adsorption rate (dq_t/dt) at higher C_0 is contributed by the larger difference of q_e and q_t at t, which gives a higher value of (q_e -q_t).

The Elovich rate equation is commonly used to represent the rapid sorption rate in the early period while the moderate rate in the later period of the sorption process. The constants a_E and the reciprocal ($1/b_E$) of constant b_E in the Elovich rate equation are related to the rate of sorption and surface coverage of adsorbent, respectively. Thus, the values of a_E as well as $1/b_E$ should increase and decrease with increasing C_0, respectively. As shown in Table 3, the sequences of values of a_E and $1/b_E$ clearly reveal that the prediction of adsorption kinetics of methomyl on MN-100 with Elovich equation satisfies the physical meanings. Together with the results of large values of R^2, Elovich rate equation obviously possesses high applicability in the prediction of adsorption kinetics of methomyl on MN-100.

CONCLUSIONS

The adsorption behavior of methomyl from aqueous solution on MN-100 has been investigated in this study. Methomyl is not stable in the basic solution (pH > 8). A lower pH value of solution gives a higher adsorption capacity of methomyl on MN-100. Both Langmuir and Freundlich adsorption isotherms can well describe the adsorption equilibrium of methomyl on MN-100, while the former possesses greater agreement with the experimental data at higher concentration range. The applicabilities of simple kinetic models (i.e., Lagergren pseudo-first-order, pseudo-second-order and Elovich rate equations) have been tested in this study. Pseudo-second-order and Elovich rate equations successfully predict the adsorption kinetics of methomyl on MN-100. Both model fittings possess satisfactorily large determination coefficients with the values of parameters consistent with the physical meanings of the models.

ACKNOWLEDGMENTS

The authors thank for the National Science Council of Taiwan for the financial support under Grants NSC 94-2211-E-002-018 and NSC 95-2221-E-002-019, and the Powder Technology Laboratory of Chemical Engineering Department of National Taiwan University for the assistance in powder characterization.

REFERENCES

1. Börner, H., Pesticides in Ground and Surface Water in Chemistry of Plant Protection. Spring-Verlag GmbH, Berlin, Germany (1994).
2. Smulders, C.J.G.M., T.J.H. Bueters, R.G.D.M. Van Kleef and H.P.M. Vijverberg, Selective effects of carbamate pesticides on rat neuronal nicotinic acetylcholine receptors and rat brain acetylcholinesterase. Toxicol. Appl. Pharmacol., 193(2), 139-146 (2003).
3. Drinking Water Directive (DWD) of European Community, Council Directive, 98/83/EC, http://ec.europa.eu/environment/water/water-drink/index_en.html (March 2007).
4. Ruhl, M.J., Recover VOCs via adsorption on activated carbon. Chem. Eng. Prog., 89(7), 37-41 (1993).
5. Tien, C., Adsorption Calculations and Modeling. Butterworth-Heinemann, Boston, MA (1994).
6. Bansal, R.C., J.B. Donnet and F. Stoeckli, Active Carbon. Marcel Dekker Inc., New York (1988).
7. Chang, C.F., C.Y. Chang and W.T. Tsai, Adsorption equilibrium of polyethylene glycol in electroplating solution on activated carbon. J. Colloid Interf. Sci., 232(1), 207-209 (2000).
8. Chang, C.F., C.Y. Chang and W. Hoell, Adsorption behavior of 2-Naphthalenesulfonate on activated carbon from aqueous systems. Ind. Eng. Chem. Res., 42(26), 6904-6910 (2003).
9. Chang, C.F., C.Y. Chang and W. Hoell, Investigating the adsorption of 2-Mercaptothiazoline on activated carbon from aqueous systems. J. Colloid Interf. Sci., 272(1), 52-58 (2004).
10. Chang, C.F., C.Y. Chang, K.H. Chen, W.T. Tsai, J.L. Shie and Y.H. Chen, Adsorption of naphthalene on zeolite from aqueous solution. J. Colloid Interf. Sci., 277(1), 29-34 (2004).
11. Chang, C.F., C.Y. Chang, W. Hoell, M. Ulmer, Y.H. Chen and H.J. Gross, Adsorption kinetics of polyethylene glycol from aqueous solution onto activated carbon. Water Res., 38(10), 2559-2570 (2004).
12. Chang, C.Y., W.T. Tsai, C.H. Ing and C.F. Chang, Adsorption of polyethylene glycol (PEG) from aqueous solution onto hydrophobic zeolite. J. Colloid Interf. Sci., 260(2), 273–279 (2003).
13. Den, W., H.C. Liu, S.F. Chan, K.T. Kin and C.P. Huang, Adsorption of phthalate esters with multiwalled carbon nanotubes and its application. J. Environ. Eng. Manage., 16(4), 275-282 (2006).
14. Diaz-Flores, P.E., R. Leyva-Romos, J.R. Rangel-Mendez, M.M. Ortiz, R.M. Guerrero-Coronado and J. Mendoza-Barron, Adsorption of 2,4-dichlorophenoxyacetic acid from aqueous solution on activated carbon cloth. J. Environ. Eng. Manage., 16(4), 249-257 (2006).
15. Isabel, R., Temperature Dependence of the Kinetics of Activated Carbon Adsorption. Internship Work Performed at Heinrich-Sontheimer-Laboratory, DVGW-Technologiezentrum Wasser, Karlsruhe, Germany (1998).
16. Karanfil, T. and J.E. Kilduff, Role of granular activated carbon surface chemistry on the adsorption of organic compounds. 1. Priority pollutants. Environ. Sci. Technol., 33(18), 3217-3224 (1999).
17. Sontheimer, H., J.C. Crittenden and R.S. Summers, Activated Carbon for Water Treatment. DVGW-Forschungsstelle, Karlsruhe, Germany (1998).
18. Tsyurupa, M.P., L.A. Maslova, A.I. Andreeva, T.A. Mrachkovskaya and V.A. Davankov, Sorption of organic compounds from aqueous media by hyper-crosslinked polystyrene sorbents Styrosorb. React. Polym., 25(1), 69-78 (1995).
19. Streat, M. and L.A. Sweetland, Physical and

adsorptive properties of Hypersol-Macronet™ polymers. React. Funct. Polym., 35(1-2), 99-109 (1997).
20. Streat, M. and L.A. Sweetland, Removal of pesticides from water using hypercrosslinked polymer phases: Part 1 - Physical and chemical characterization of adsorbents. Process Saf. Environ., 76(B2), 115-126 (1998).
21. Streat, M. and L.A. Sweetland, Removal of pesticides from water using hypercrosslinked polymer phases: Part 2 - Sorption studies. Process Saf. Environ., 76(B2), 127-134 (1998).
22. Streat, M., L.A. Sweetland and D.J. Horner, Removal of pesticides from water using hypercrosslinked polymer phases: Part 3 - Mini-column studies and the effect of fulvic and humic substances. Process Saf. Environ., 76(B2), 135-141 (1998).
23. Streat, M., L.A. Sweetland and D.J. Horner, Removal of pesticides from water using hypercrosslinked polymer phases: Part 4 - Regeneration of spent adsorbents. Process Saf. Environ., 76(B2), 142-150 (1998).
24. Tai, M.H., B. Saha and M. Streat, Characterisation and sorption performance of a Hypersol-Macronet polymer and an activated carbon. React. Funct. Polym., 41(1-3), 149-161 (1999).
25. Council of Agriculture of Taiwan (COAT); http://bulletin.coa.gov.tw/index_intro.php (July 2006).
26. Chang, C.F., C.Y. Chang and W.T. Tsai, Effects of burn-off and activation temperature on preparation of activated carbon from corn cob agrowaste by CO_2 and steam. J. Colloid Interf. Sci., 232(1), 45-49 (2000).
27. Braunauer, S., L.S. Deming, W.S. Deming and E. Teller, On a theory of the van der Waals adsorption of gases. J. Am. Chem. Soc., 62(7), 1723-1732 (1940).
28. Lowell, S. and J.E. Shields, Powder Surface Area and Porosity. 3rd Ed., Chapman & Hall, New York (1991).
29. Toxic Data Network, National Library of Medicine. http://toxnet.nlm.nih.gov/ (2006).
30. Cussler, E.L., Diffusion: Mass Transfer in Fluid Systems. Cambridge University Press, New York (1997).
31. Ho, Y.S. and G. Mckay, A comparison of chemisorption kinetic models applied to pollutant removal on various sorbents. Process Saf. Environ., 76(B4), 332-340 (1998).
32. Low, M.J.D., Kinetics of chemisorption of gases on solids. Chem. Rev., 60(3), 267-312 (1960).
33. Sposito, G., The Surface Chemistry of Soils. Oxford University Press, New York (1984).

Discussions of this paper may appear in the discussion section of a future issue. All discussions should be submitted to the Editor-in-Chief within six months of publication.

Manuscript Received: March 9, 2007
Revision Received: June 4, 2007
and Accepted: June 15, 2007